Rigorous treatment of first-principles data for quasiharmonic thermodynamics of solids

A. Otero-de-la-Roza and V. Luaña

Departamento de Química Física y Analítica, Facultad de Química, Universidad de Oviedo, 33006 Oviedo, Spain
(Dated: April 29, 2011)

The quasiharmonic approach to the *ab initio* calculation of thermodynamic properties in crystals is revisited with the improvement of two significant aspects: i) the use of averaged strain polynomials is proposed to reduce the uncertainty in the fitting of energy *vs.* volume data, and provide statistical measure of the errors introduced by the fit and ii) the systematic error of the calculations due to the approximate nature of the exchange and correlation functional is repaired through an empirical energy correction scheme that, based only in two experimental parameters, the equilibrium volume and bulk modulus, brings the calculated thermodynamic properties into agreement with the experimental measurements on a extremely wide range of pressures and temperatures. The proposed procedure is simple, systematic and applicable to any solid.

I. INTRODUCTION

We present a simple, systematic and general method to calculate *ab initio* thermodynamic properties of a solid at arbitrary pressures and temperatures, with an accuracy that rivals experimental measurements. The procedure described is based on the quasiharmonic approximation (QHA), a mainstream route to access the thermodynamics of a solid, that requires the computation of the volume-dependent static energy and phonon density of states (phDOS), either using the direct method[1,2] or the Density Functional Perturbation Theory (DFPT)[3]. However, we show in this article that the steps leading from these basic data to the final thermodynamic properties require a careful treatment for being able to blindly (i.e. without experimental confirmation) predict the properties of a solid. The discussion is structured around two main ideas.

First, the equations of state (EOS) used to model the static and free energy *versus* volume data are adapted from the experimental field (for instance, Vinet, BM3,...). While the purpose of those EOS is to extrapolate the crystal behavior to a range of pressures and temperatures wider than that of the experience, our objective is the interpolation and calculation of energy derivatives. We show how averages of strain polynomials provide an excellent tool for this purpose.

Second, the main source of error in DFT based calculations is the approximate exchange-correlation functional. Lacking the correct functional or a systematic way to improve it, we turn to an empirical correction where only two easily accesible experimental data (room temperature volume and bulk modulus) are needed. The correction modifies the static energy, and therefore the calculated $V(p,T)$ but not the volume-dependent phDOS. As a result, the agreement with experimental results is much improved in a wide range of pressures and temperatures.

Our discussion will be centered on periclase, the rock salt phase of magnesium oxide. A major component of the Earth's mantle, industrially relevant ceramic, stable in the rock salt phase for a wide pressure and temperature range, MgO has become one of the most studied materials in this field[4–9]. Apart from its value as benchmark, the detailed knowledge of its $p(V,T)$ equation of state (EOS) is of fundamental importance for its role as a calibration sample in high-pT diffraction studies, and is still the subject of a lively debate[7]. We show later that, using our procedure, a first principles EOS can be proposed.

II. COMPUTATIONAL DETAILS

The *ab initio* calculations have been done under the plane-wave pseudopotentials approach[10], using ultrasoft pseudopotentials[11] for Mg $(2s^2p^63s^1)$ and O $(2s^1p^5)$. Exchange and correlation effects have been introduced using the LDA and GGA approximations in the Perdew and Zunger[12] and Perdew-Burke-Erzenhof[13] parametrizations, respectively. The energies and the phDOS have been checked for convergence with respect to the relevant calculation parameters: plane-wave cutoff energy (80 Ry), electronic $\boldsymbol{k}$-mesh (Monkhorst-Pack, MP, $4\times4\times4$) and vibrational $\boldsymbol{q}$-mesh (MP $6\times6\times6$). The techniques described in the next section are implemented in the GIBBS2 program[14–16].

III. A PROCEDURE FOR ACCURATE *AB INITIO* THERMODYNAMICS

The thermodynamic behavior of solids is determined, under hydrostatic conditions, by the generalized Gibbs energy

$$G^\star(\boldsymbol{x}, p, T) = E_{\text{sta}}(\boldsymbol{x}) + pV(\boldsymbol{x}) + F^\star_{\text{vib}}(\boldsymbol{x}, T) \quad (1)$$

where $\boldsymbol{x}$, the free geometry, is limited in this case to the cell volume, V, by the symmetry of the rock-salt phase, the *static* energy is the direct result of the electronic

TABLE I. Equilibrium properties of MgO determined from several fittings to the same GGA theoretical calculations. The results correspond to the static model. The avX models correspond to an average of polynomials of degree 2 to 12 in the eulerian (avBM), natural (avPT), lagrangian (avLagr), and infinitesimal strain (avInf).

	V_0 (bohr^3)	B_0 (GPa)	B_0'	B_0'' (GPa^{-1})
BM3	129.6757	158.70	3.9457	−0.0242
BM4	130.0741	151.23	4.1001	−0.0279
Vinet	130.7726	132.25	4.8306	−0.0584
AP2	130.0648	147.98	4.3026	−0.0367
avBM	130.0792(50)	150.49(26)	4.1284(91)	−0.0266(22)
avPT	130.0839(115)	150.34(24)	4.1284(169)	−0.0246(35)
avLagr	130.0806(205)	150.20(44)	4.1428(562)	−0.0237(139)
avInf	130.0815(49)	150.39(22)	4.1290(94)	−0.0255(31)

structure DFT calculation, and the vibrational contribution to the Helmholtz energy is given in the QHA approach by

$$F_{\text{vib}}^{\star} = \int_0^{\infty} g(\omega, \boldsymbol{x}) \left[\frac{\hbar\omega}{2} + k_B T \ln\left(1 - e^{-\hbar\omega/k_B T}\right) \right] d\omega \tag{2}$$

where $g(\omega, \boldsymbol{x})$, the phDOS, depends on the crystal geometry. Further contributions to the free energy can be ignored for the insulating, diamagnetic, ideal MgO crystal.

Fitting analytical EOS to $E(V)$ and $F^*(V;T)$ data is a fundamental step in the determination of the equilibrium properties at fixed temperature and in obtaining the derivatives required to model the thermal behavior. Up to the third or fourth derivative of $E(V)$ are required, a strict test on the representation of the discrete set of theoretical energy values.

At present, the usual way in the literature is to follow experimental practice: an analytical form with a few parameters is fitted non-linearly[5,6]. Birch-Murnaghan of orders 3 and 4, Vinet[17,18] and Holzapfel's AP2[19,20] forms are among the most popular representations of the cold isotherm data. Table I shows that this non linear fitting step introduces a significant uncertainty. Equilibrium bulk modulus from 132 to 159 GPa, or B_0' values from 3.9 to 4.8 can be used on equal footing according to Table I.

This uncertainty, that is readily transferred into the thermal calculation, is an artifact of the fitting procedure. The theoretical $E(V)$ (a 129 point volume grid, in the range 72–143 bohr^3) is smooth enough to produce a much improved precision under an adequate statistical treatment of the fitting. Our method, described with detail in ref. 15 and 21, expands the energy as strain polynomials of arbitrary order:

$$E_n(f) = \sum_{k=0}^{n} c_k f^k \tag{3}$$

where f is one of many possible generalized strains[22]. For instance, the Birch-Murnaghan (BM)[23–25] EOS of

order n would be the result of using an eulerian strain: $f = (x^{-2/3} - 1)/2$, where $x = V/V_r$ is the cell compression and V_r is any positive reference volume. Similarly, the natural ($f = (1/3)\ln x$), lagrangian ($f = [x^{2/3} - 1]/2$) and infinitesimal ($f = (1 - x^{-1/3})$) strains would give rise to the Poirier-Tarantola (PT)[26], Thomson[27], and Bardeen[28] families of EOS, respectively.

In the traditional treatment the low order EOS are deduced by imposing $V \rightarrow V_0$, $V d^2E/dV^2 \rightarrow B_0$, $dB/dP \rightarrow B_0',...$ in the limit $f \rightarrow 0$, thus giving rise to complex expressions for the c_k coefficients. The equilibrium properties (V_0, B_0, $B_0',...$) are treated as the fitting parameters. However, it turns out that the direct non-linear optimization of these quantities is difficult in the absence of good starting parameters because of their strong correlation. This makes fits of higher order in the strain unattainable.

In our approach, the c_k coefficients are determined by a linear fit of the $E_n(f)$ polynomial to the $E(V)$ or $F(V)$ data. Linear polynomial fits are robust to very high degress, pose no convergence problems and allow a straightforward statistical measure of the goodness of the fit. Furthermore, each polynomial of a given degree n can be assigned a normalized weight to produce an average polynomial by convex linear combination. In addition, error bars obtained as a standard deviation of the calculated properties can be assigned. After a number of tests, we have opted for the weights $P_n = e^{-w_n}/\sum_i e^{-w_i}$ where $w_n = N_n \mathcal{S}_n/(n \mathcal{S}_{\text{min}})$, N_n is the number of points fitted, $\mathcal{S}_n$ the sums of squares of residuals and $\mathcal{S}_{\text{min}} = \min_n \mathcal{S}_n$. With these weights, the polynomials that achieve the better fits using less coefficients have larger contributions to the average.

Table I reports the static equilibrium properties of MgO obtained using the polynomial averaging scheme. The four strain definitions produce results equivalent within their respective error bars. In particular, B_0, B_0', and B_0'' are consistent among the different fittings. The B_0''' and higher derivatives have error bars similar or larger that their average values. The BM average is used for the rest of the article.

A number of numerical experiments[15,21] has been undertaken to check the relevance of the error bars: reducing and enlarging the data set (from 17 to 2049 points) and the volume range (up to 10–320 bohr^3). The predicted equilibrium properties remained stable in all the tests. Furthermore, to base the described procedure on a firmer statistical foundation, we have conducted a bootstrap analysis[29] by sampling from 100 to 10^6 random subsets of the 129-point dataset, fitting fixed-order polynomials and doing an statistical analysis of the results. The error bars proposed in the previous paragraph are more conservative than those of the bootstrap method, the latter being usually three or more times smaller than the former. Therefore, our error bars significantly measure the precision with which the thermodynamic properties are calculated.

We now turn to the problem of finding an energy cor-

TABLE II. Thermodynamic properties of MgO at 298.15 K and 1,000 K. Most experimental values are from the compilation by Anderson and Zou[30]. Room temperature V and B_T (**boldface** in the table) are from Li *et al.*[8]. The theoretical error bars within parenthesis are inherited from the EOS fitting error.

| | Room temperature (0 GPa and 298.15 K) | | | | | (0 GPa and 1000 K) | |
	PBE	LDA	PBEcorr	LDAcorr	expt.	PBEcorr	expt.
V (bohr^3)	132.377(33)	123.155(69)	126.024(19)	126.026(74)	**126.025**	129.708(84)	129.6
F_{vib} (kJ/mol)	9.9613(72)	11.227(16)	11.4236(47)	10.554(18)		-31.613(59)	
S (J/mol K)	29.919(15)	27.343(32)	27.0028(88)	28.670(36)	27.18	82.853(56)	82.24
p_{th} (GPa)	2.534(30)	2.722(29)	2.624(15)	2.701(28)	*0.717*	6.943(67)	*4.96*
B_T (GPa)	141.30(56)	161.84(70)	161.43(50)	161.31(60)	**161.3**	141.2(20)	141
B_S (GPa)	143.87(56)	164.27(70)	163.72(50)	163.93(60)	163.9	151.6(20)	151.1
α (1×10^{-5} K)	3.733(16)	3.237(16)	3.1002(97)	3.361(15)	3.12	4.680(68)	4.47
C_v (J/mol K)	38.1863(71)	36.918(17)	36.6821(50)	37.619(18)	36.9	48.5530(28)	47.61
C_p (J/mol K)	38.8799(97)	37.473(21)	37.2023(57)	38.231(21)	37.409	52.132(55)	50.87
B'_T	4.297(42)	4.251(57)	4.173(43)	4.279(71)		4.53(12)	
B''_T (GPa^{-1})	-0.054(10)	-0.0366(60)	-0.0333(28)	-0.0390(73)		-0.089(24)	
γ	1.63186(59)	1.5597(14)	1.53435(24)	1.6209(17)	1.54	1.5751(11)	1.54

rection to rectify the known systematic deviations in DFT static energies. The need for a correction is widely acknowledged[31–33] but few systematic studies of different models have been reported[31,33]. After trying several expressions, we settled for a correction based on Kunc and Syassen's observation[32] that static p/B_0 *vs.* V/V_0 curves closely match for LDA, GGA and experimental results. The proposed empirical energy correction (EEC) modifies the the static energy in eq. 1 according to

$$\tilde{E}_{\text{sta}}(V) = E_{\text{sta}}(V_0) + \frac{B_{\text{exp}}V_{\text{exp}}}{B_0 V_0} \left[E_{\text{sta}} \left(\frac{VV_0}{V_{\text{exp}}} \right) - E_{\text{sta}}(V_0) \right] \quad (4)$$

where (V_0, B_0) are calculated static equilibrium properties, $(V^0_{\text{exp}}, B^0_{\text{exp}})$ are experimental properties at room conditions, and $(V_{\text{exp}}, B_{\text{exp}})$ would correspond to the experimental properties once corrected for hypothetical static conditions. To determine the latter we use the conditions

$$\frac{\partial G^*}{\partial V}(V^0_{\text{exp}}; 0, T^0) = 0, \quad V \frac{\partial^2 F^*_{\text{vib}}}{\partial V^2}(V^0_{\text{exp}}, T^0) = B^0_{\text{exp}} \quad (5)$$

where $T^0 = 298.15$ K. This leads to:

$$\frac{B_{\text{sta}}(fV_0)}{p_{\text{sta}}(fV_0)} = \frac{B^0_{\text{exp}} - B_T(V^0_{\text{exp}}, T^0) + B_{\text{sta}}(V^0_{\text{exp}})}{p_{\text{th}}(V^0_{\text{exp}}, T^0)} \quad (6)$$

where $p_{\text{sta}} = -dE_{\text{sta}}/dV$ and $p_{\text{th}} = -\partial F^*/\partial V$ are the static and thermal contributions to the pressure, and B_T is the isothermal bulk modulus and p_{th} is the thermal pressure. The scaling factor $f = V^0_{\text{exp}}/V_{\text{exp}} > 1$ is the only unknown quantity in eq. 6, and is easily found by bracketing and bisection. Once f is obtained, we have:

$$V_{\text{exp}} = \frac{V^0_{\text{exp}}}{f}, \quad B_{\text{exp}} = -B_0 \frac{p_{\text{th}}(V^0_{\text{exp}})}{p_{\text{exp}}(fV_0)} \quad (7)$$

and the eq. 4 can be applied. An important point is that the static energy, and therefore the calculated $V(p,T)$

is modified, but not the phDOS associated to each volume. As a consequence, other properties (magnetic, electronic,...) calculated as derivatives of the DFT total energy and that depend strongly on the volume could benefit from the application of EECs as well.

An important observation is that EECs correct the Gibbs free energy, $G(p,T)$, of a solid and, when more than one phase is considered, also the phase diagram. Whenever experimental data for the phases involved is available, the EEC proposed in this article is directly applicable to each phase. However, in many cases, V^0_{exp} and B^0_{exp} are not experimentally accessible for a thermodynamically metastable phase. In such cases, two generalizations of the procedure above are possible:

1. Equations 4 to 7 can be easily modified to accept experimental volume and bulk modulus data at arbitrary pressures and temperatures, rather than ambient conditions. It is also possible to propose equations simpler than 4 to correct the static energy, using only the experimental volume at given p and T conditions.

2. When even this solution is not feasible, the coefficients entering equation 4 can be transferred from the stable phase to the rest of the phases in the diagram. Although a detailed study is necessary, it is encouraging that, as shown by van de Walle and Ceder[31], the pressure required to correct the static equilibrium volume using a simple pV scaling can be expressed as a concentration average of elemental pressures. This observation points to the systematic DFT errors being linked primarily to the atomic composition—not the geometry— of the phase, thus favoring the transferability of the correction coefficients.

We are currently exploring both possible generalizations of the EEC.

IV. RESULTS

Table II reports the thermodynamic properties predicted at room temperature by the LDA and PBE calculations before and after the EEC correction has been applied. As usual, LDA overbinds and PBE underbinds with respect to the experiment. LDA is, in this crystal, rather close to most of the experimental properties, that have been obtained from the compilation by Anderson and Zou[30]. This coincidence, that extends to other similar crystals, explains the popularity of LDA for ionic compounds. The EEC works as expected, converging the predictions of both LDAcorr and PBEcorr towards the experiment. The correction is, in general, highly successful, and slightly better in the case of PBEcorr. The noticeable exception is the thermal pressure, p_{th}, some 2 GPa larger according to our calculations than the values reported in Ref. 30, where it was indirectly calculated from other experimental values.

The agreement of PBEcorr results with the experiments extends to high temperatures, and Table II compares the 1000 K properties as an example. Our results show that the correction of the static energy is enough to predict excellent thermodynamic properties on a large range of temperature and pressure conditions, allowing the corrected QHA results to blindly predict the behavior of the crystals in regions uncharted or off the experimental limits.

To determine how large this range is we have examined carefully the behavior of the two most critical magnitudes, V and B, with both p and T. The results are collected in Fig. 1 and compared to the high quality experimental dataset recommended by Tange *et al.*[7]. The thermal expansion data were obtained by Dubrovinsky and Saxena[36], Fiquet et al.[34] and Sinogeikin et al.[35] using X-ray diffraction and wire-heated multi-anvil cells. Additional $B_S(T)$ data were obtained from a compilation of previous work by Anderson[30]. The isothermal data are provided by experiments that avoid the use of an external pressure calibrant: X-ray diffraction coupled with Brillouin scattering (DAC, ref. 9) or ultrasonic interferometry (multi-anvil, ref. 8) experiments provide the isothermal data. For comparison, we include the raw results by Speziale[4], a popular MgO equation of state for diffraction experiments, obtained using the ruby pressure scale. Our data has been corrected with the expression in equation 4, using data from Li et al.[8]: $V_{\text{exp}}^0 = 126.025$ bohr^3 and $B_{\text{exp}}^0 = 161.3$ GPa.

The $V(p, 300\ K)$ plot shows that LDAcorr, PBEcorr and the experimental data are indistinguishable up to the pressure where the experiments are reliable. In addition, the theoretical results agree up to 250 GPa with differences smaller than 0.05 bohr^3. A similar agreement is obtained for $B_S(p, 300\ K)$, whose computation is more involved than the equilibrium volume. In this case, the uncorrected LDA results also coincide with LDAcorr, PBEcorr and the experiment. The agreement between the theoretical B_S extends to 250 GPa with differences

TABLE III. Pressure-volume-temperature results for MgO, using the PBE functional and corrected with the experimental volume ($V_0 = 126.025$ bohr^3) and bulk modulus (161.3 GPa). Each column represents a temperature, given in the first entry (Kelvin). Pressures (in GPa) are presented against compression, $x = V/V0$.

x	298.15	500	1000	1500	2000	2500	3000
1.000	0.00	1.14	4.33	7.65	11.01	14.37	17.71
0.975	4.31	5.43	8.61	11.92	15.26	18.62	21.93
0.950	9.22	10.32	13.48	16.78	20.12	23.48	26.76
0.925	14.82	15.89	19.03	22.33	25.67	29.02	32.28
0.900	21.20	22.25	25.37	28.66	31.99	35.34	38.59
0.875	28.49	29.52	32.61	35.89	39.22	42.56	45.81
0.850	36.83	37.83	40.90	44.16	47.48	50.82	54.07
0.825	46.38	47.36	50.39	53.65	56.95	60.29	63.55
0.800	57.35	58.30	61.31	64.55	67.85	71.18	74.47
0.775	69.98	70.90	73.88	77.11	80.42	83.75	87.07
0.750	84.54	85.43	88.39	91.63	94.94	98.28	101.65
0.725	101.38	102.25	105.20	108.45	111.78	115.15	118.56
0.700	120.91	121.76	124.71	127.98	131.35	134.76	138.24
0.675	143.64	144.47	147.42	150.74	154.16	157.62	161.18
0.650	170.17	170.98	173.95	177.33	180.81	184.35	187.98
0.625	201.24	202.04	205.03	208.47	212.04	215.66	219.38
0.600	237.81	238.59	241.61	245.11	248.76	252.47	256.28
0.575	281.02	281.77	284.81	288.38	292.12	295.92	299.82
0.550	332.32	333.05	336.08	339.71	343.52	347.41	351.39
0.525	393.60	394.29	397.30	400.97	404.85	408.82	412.86
0.500	467.19	467.84	470.81	474.50	478.44	482.47	486.57

smaller that 2 GPa.

The $V(T)$ and $B_S(T)$ curves at 0 GPa in fig. 1 should help us determine when the QHA fails due to anharmonic effects. Anharmonicity tends to decrease its relative importance as the pressure increases, so the 0 GPa curves represent a worst-case scenario in this respect. The agreement of the PBEcorr results with the experiment is excellent, even at 2000 K. As a comparison, LDAcorr starts to differ from the experimental $V(T)$ curve around 1000 K, and from the $B_S(T)$ curve even earlier.

Our results compare well with the best available EOS in the literature, even at very high temperature. As an example the fig. 2 shows the 3000 K isotherm, just a bit below the melting temperatute (3125 K). The EOS by Speziale *et al.*[4] and by Tange *et al.*[7] are built from experimental measurements and empirical extrapolations. The EOS by Speziale, in particular, is currently used as a pressure scale in high pT diffraction experiments. Wu et al.[6] use QHA theoretical results to extrapolate the data by Speziale *et al.* to higher pressures. Our PBEcorr results agree with the three other datasets, even in the low p and high T region where the intrinsic anharmonic corrections, not included in our work, should be most important. The comparison with Wu *et al.*[6] results is particularly relevant: our fundamental theoretical calculation is equivalent to theirs but, whereas they extrapolate the experimental $p(V)$ data by Speziale *et al.*, we use only two experimental data, our procedure can be applied to an arbitrary crystal, and is at least as effec-
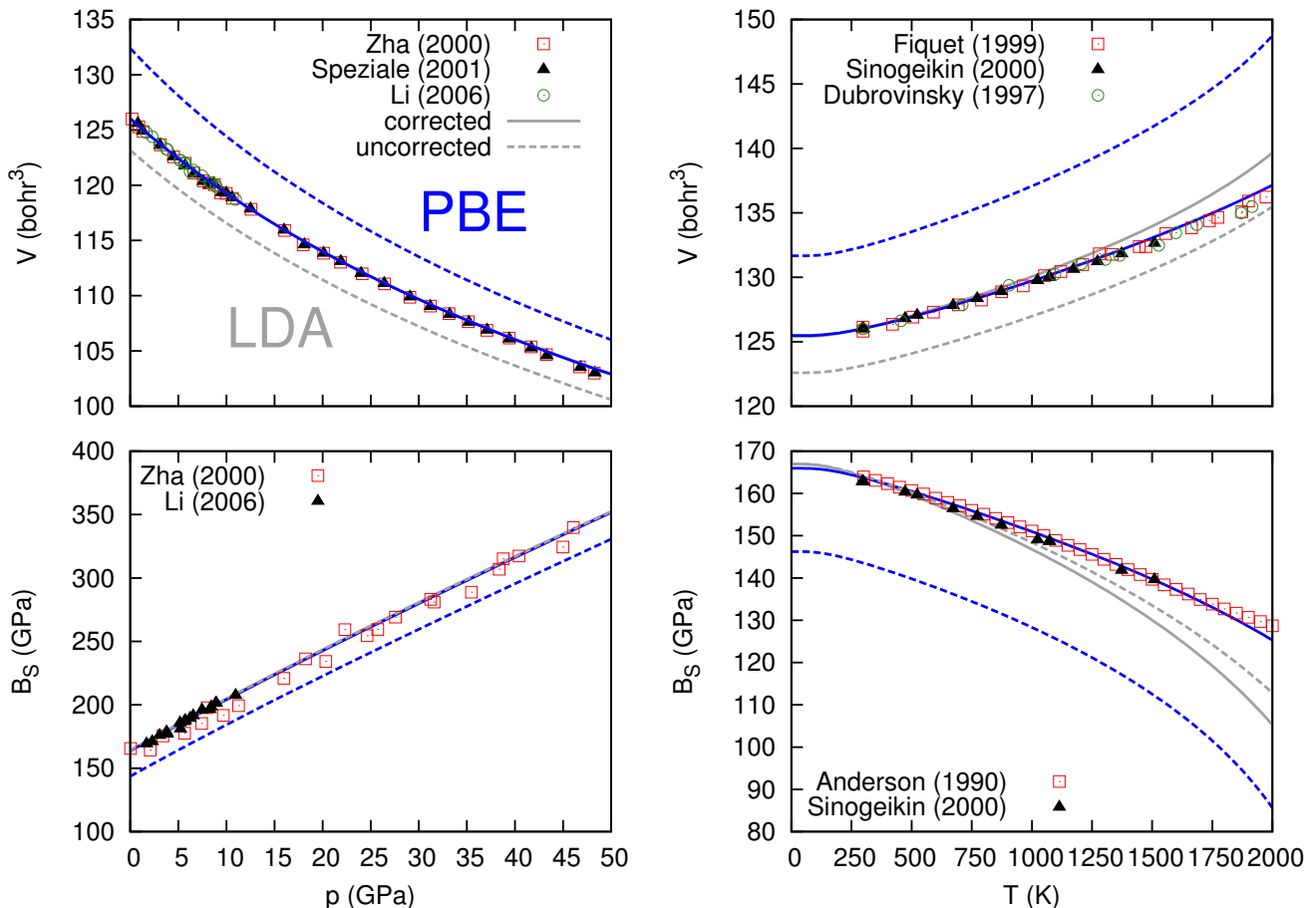
FIG. 1. Corrected (solid lines) and uncorrected (stippled) MgO results using LDA (light gray) and PBE (dark blue) functionals. Our results are compared to a high quality experimental dataset, particularly experiments that avoid the use of an external pressure calibrant[8,9,34–36]. Speziale *et al.*[4] data, based on the ruby scale, is also included due to its popularity. Additional $B_S(T)$ data from ref.[30] have also been included.
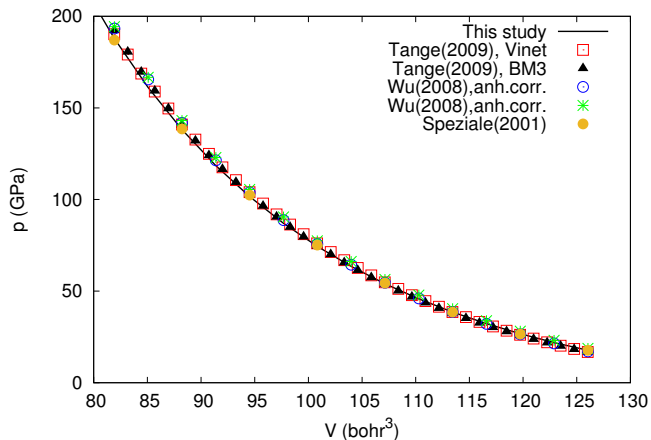

FIG. 2. 3000 K isotherm of MgO.

tive. An exhaustive tabulation of the calculated p-V-T equation of state is presented in table III.

As a final result, figure 3 shows the predicted phase diagram in the low temperature region encompassing the

B1→B2 transition. The B2 phase has not been observed experimentally[37] so there are no data available for the empirical correction but, as described above, we can use the correction coefficients of the B1 phase. Even though we can not compare to experiment, it is encouraging that the 40 GPa gap in the predicted transition pressures between LDA and PBE is reduced to 5–10 GPa upon correction. The result is consistent with previous theoretical studies[38,39] that place the static transition pressure around 500 GPa.

V. CONCLUSION

We have presented a carefully designed procedure to transform static DFT energies and DFPT phDOS into thermodynamic properties that is simple, efficient, systematic and applies to arbitrary crystals. Some points about the treatment of first principles thermodynamic data have been clarified: i) using strain polynomials removes the uncertainty in the calculation of equations of state and their derivatives, and provides an statistical
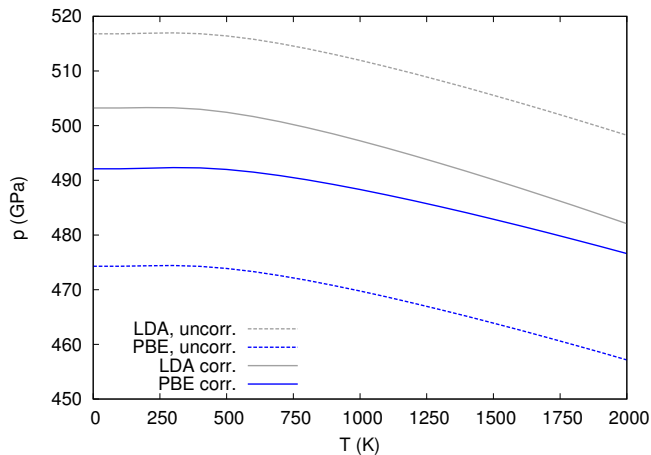
FIG. 3. Calculated temperature dependence of the B1→B2 transition pressures of magensium oxide. Corrected and uncorrected results for LDA and PBE are presented.

measure of the goodness of the fit and ii) a congruent

energy correction is necessary, and we propose one which uses two experimental data which are easily available. The combination of the two techniques has allowed us to formulate an almost fully *ab initio* equation of state of MgO that rivals in accuracy with the best $p(V,T)$ data propsed in the literature. The performance of our procedure in other test systems is also excellent, and will be the subject of further studies. Given the extraordinary agreement with the available experimental data for MgO, we expect that the corrected QHA results represent faithfully the behavior of the solid under extreme conditions, provided the limits of validity of QHA are not overstepped.

ACKNOWLEDGMENTS

[1] W. Frank, C. Elsässer, and M. Fähnle, Phys. Rev. Lett. **74**, 1791 (1995).

[2] K. Parlinski, Z. Q. Li, and Y. Kawazoe, Phys. Rev. Lett. **78**, 4063 (1997).

[3] S. Baroni, S. de Gironcoli, A. Dal Corso, and P. Giannozzi, Rev. Mod. Phys. **73**, 515 (2001).

[4] S. Speziale, C. S. Zha, T. S. Duffy, R. J. Hemley, and H. K. Mao, J. Geophys. Res. **106**, 515 (2001).

[5] A. R. Oganov and P. I. Dorogokupets, Phys. Rev. B **67**, 224110 (2003).

[6] Z. Q. Wu, R. M. Wentzcovitch, K. Umemoto, B. S. Li, K. Hirose, and J. C. Zheng, J. Geophys. Res. **113**, B06204 (2008).

[7] Y. Tange, Y. Nishihara, and T. Tsuchiya, J. Geophys. Res. **114**, B03208 (2009).

[8] B. Li, K. Woody, and J. Kung, J. Geophys. Res. **111**, B11206 (2006).

[9] C. Zha, H. Mao, and R. Hemley, Proc. Natl Acad. Sci. USA **97**, 13494 (2000).

[10] P. Giannozzi, S. Baroni, N. Bonini, M. Calandra, R. Car, C. Cavazzoni, D. Ceresoli, G. L. Chiarotti, M. Cococcioni, I. Dabo, A. Dal Corso, S. de Gironcoli, S. Fabris, G. Fratesi, R. Gebauer, U. Gerstmann, C. Gougoussis, A. Kokalj, M. Lazzeri, L. Martin-Samos, N. Marzari, F. Mauri, R. Mazzarello, S. Paolini, A. Pasquarello, L. Paulatto, C. Sbraccia, S. Scandolo, G. Sclauzero, A. P. Seitsonen, A. Smogunov, P. Umari, and R. M. Wentzcovitch, J. Phys.-Condens. Matter **21**, 395502 (2009).

[11] D. Vanderbilt, Phys. Rev. B **41**, 7892 (1990).

[12] J. P. Perdew and A. Zunger, Phys. Rev. B **23**, 5048 (1981).

[13] J. P. Perdew, K. Burke, and M. Ernzerhof, Phys. Rev. Lett. **77**, 3865 (1996).

[14] M. A. Blanco, E. Francisco, and V. Luaña, Comput. Phys. Commun. **158**, 57 (2004).

[15] A. Otero-de-la Roza and V. Luaña, Comput. Phys. Commun. (2010), (in press).

[16] A. Otero-de-la Roza, V. Luaña, and D. Abbasi, Comput. Phys. Commun. (2011), (submitted).

[17] P. Vinet, J. Ferrante, J. R. Smith, and J. H. Rose, J. Phys. C: Solid State Phys. **19**, L467 (1986).

[18] P. Vinet, J. H. Rose, J. Ferrante, and J. R. Smith, J. Phys: Condens. Matter **1**, 1941 (1989).

[19] W. B. Holzapfel, High Press. Res. **16**, 81 (1998).

[20] W. B. Holzapfel, Z. Kristall. **216**, 473 (2001).

[21] A. Otero-de-la Roza and V. Luaña, Comput. Theor. Chem. (2011), (in press).

[22] O. L. Anderson, *Equations of State for Solids in Geophysics and Ceramic Science* (Oxford UP, Oxford, UK, 1995), p. 225.

[23] F. D. Murnaghan, Proc. Natl. Acad. Sci. USA **30**, 244 (1944).

[24] F. Birch, Phys. Rev. **71**, 809 (1947).

[25] F. Birch, J. Geophys. Res. **83**, 1257 (1978).

[26] J.-P. Poirier and A. Tarantola, Phys. Earth Planet. Int. **109**, 1 (1998).

[27] L. Thomson, J. Phys. Chem. Solids **31**, 2003 (1970).

[28] J. Bardeen, J. Chem. Phys. **6**, 372 (1938).

[29] R. R. Wilcox, *Fundamentals of Modern Statistical Methods*, 2nd ed. (Springer, New York, USA, 2010), p. 278.

[30] O. Anderson and K. Zou, J. Phys. Chem. Ref. Data **19**, 69 (1990).

[31] A. van de Walle and G. Ceder, Rev. Mod. Phys. **74**, 11 (2002).

[32] K. Kunc and K. Syassen, Phys. Rev. B **81**, 134102 (2010).

[33] A. B. Alchagirov, J. P. Perdew, J. C. Boettger, R. C. Albers, and C. Fiolhais, Phys. Rev. B **63**, 224115 (2001).

[34] G. Fiquet, D. Andrault, J. P. Iti, P. Gillet, and P. Richet, Phys. Earth Planet. Int. **95**, 1 (1996).

[35] S. V. Sinogeikin, J. M. Jackson, B. O'Neill, J. W. Palko, and J. D. Bass, Rev. Sci. Instrum. **71**, 201 (2000).

[36] L. S. Dubrovinsky and S. K. Saxena, Phys. Chem. Minerals **24**, 547 (1997).

[37] T. S. Duffy, R. J. Hemley, and H. K. Mao, Phys. Rev. Lett. **74**, 1371 (1995).

[38] A. R. Oganov and P. I. Dorogokupets, Phys. Rev. B **67**, 224110 (2003).

[39] A. B. Belonoshko, S. Arapan, R. Martonak, and A. Rosengren, Phys. Rev. B **81**, 054110 (2010).